Air Quality Deterioration in a Pristine Area due to a Petroleum Refinery and Associated Activities

Devolakshi Handique and Krishna G. Bhattacharyya[*]

Department of Chemistry, Gauhati University, Guwahati 781014, India

*Corresponding author. Tel: +91-9864031987, E-mail: kgbhattacharyya@gmail.com

ABSTRACT

The work describes an assessment of the major air pollutants, NO_2, SO_2, CO, O_3, NH_3, coarse and fine particulate matter (PM_{10}, $PM_{2.5}$) in ambient air in and around a 3 million tonne Petroleum Refinery and the possible impacts on a pristine area marked by the presence of the world-famous Kajiranga National Park, a world heritage site and habitat for the most number of one-horned rhinos in the world. The Refinery is at an aerial distance of 20-25 km from the wildlife habitat. The assessment is based on regular monitoring at four stations around the Refinery and one station near the National Park. Heavy rains during June to August influence the pollutant concentrations while at other times of the year, large traffic volume adds to the pollutant concentrations that peak during November to March, the dry months of the year. Correlation analysis by scatter technique is utilised to obtain the enhancement ratios to predict the variations in the concentrations of the pollutants and their spatial distribution. Computation of air quality index (AQI) indicates that the coarse and the fine particulates in the ambient air could be a major hazard to wildlife in the area.

Key words: PM_{10} and $PM_{2.5}$, Petroleum refinery impacts, Wildlife habitat, Enhancement ratios, Air quality index

1. INTRODUCTION

Ambient air loaded with pollutants, either particulates or gases, has become a critical problem throughout the world because of the serious impact of the pollutants on health of all life-forms and on natural biodiversity, particularly related to wild animals (Akimoto, 2003). For a long time, the ambient air quality in urban and semi-urban areas of the world has been affected by the use of coal for domestic heating and electricity generation, and fuel oil for the boilers and also for power generation (OECD, 2008). Increasing combustion of fossil fuels in vehicles and in industries is having major impacts on the air quality. The pollutants, carbon monoxide (CO), sulphur dioxide (SO_2), nitrogen oxides (NO_x), ozone (O_3), hydrocarbons (HC) and particulate matter (PM) depending on their chemical composition, reactivity, emission volumes, meteorological conditions, life time in the atmosphere, accumulation, diffusion and transport properties over long and short distances have affected the living conditions in many places (Kampa and Castanas, 2008). Secondary interactions like those under the influence of sunlight produce more harmful pollutants like ozone, depending on the solar radiation intensity, absolute and relative concentrations of species like NO_x and Volatile Organic Compounds, and atmospheric temperature (Pudasainee *et al*., 2006; Nisanth *et al*., 2012). While the impacts of the air pollutants on human health have received much attention, this has not been the case with the wildlife habitats.

A Petroleum Refinery is a varied source of emission of a number of primary and secondary pollutants to the atmosphere. For example, the vacuum distillation unit (VDU) of a refinery is a major emitter of SO_2, while the crude distillation unit (CDU) emits almost all major air pollutants, SO_2, NO, NO_2, CO, etc. (Shtripling and Bazhenov, 2015). These and other gases also come to the atmosphere in the form of fugitive emissions from the joints and leaks in the huge refinery system. In a recent report, the monetary damages arising from exposure to fine particulate matter ($PM_{2.5}$), sulphur dioxide (SO_2), nitrogen oxides (NO_x), ammonia (NH_3), and volatile organic compounds (VOC) from the energy sector industry including oil refineries have been estimated and it has been found that the loss is huge and that SO_2 is a major contributor to the damages (Jaramillo and Muller, 2016). With the concern over climate change and global warming, modern refineries are trying to develop built-in CO_2-capture mechanism in order to introduce control over gas emissions from

various refinery processes (Heal and Kemp, 2013). New scientific evidence has led to a recognition of the significant role of black particles (black carbon - BC) as short-lived climate forcers. Measures, focused on these particles and methane, are expected to achieve a significant short-term reduction in global warming. If they were to be implemented immediately, together with measures to reduce CO_2 emissions, the chances of containing the earth's temperature increase to less than 2°C relative to pre-industrial levels are likely to improve (UNEP, 2011). The same measures would also directly benefit global health and food security.

Because of its longer lifetime, CO can be used to determine the state of local and regional air pollution including the oxidation processes in the atmosphere and to monitor the extent of biomass burning in an area (Edwards *et al.*, 2006). The atmosphere is cleansed of CO by reaction with OH radicals, the most abundant cleaning agent during the day (Duncan *et al.*, 2007). Apart from contributions from biomass burning and fossil fuel use, almost 50% of CO in the atmosphere arises from oxidation of CH_4 and volatile organic compounds (VOCs) (Logan *et al.*, 1981). It is important to keep the CO concentration in check because of its extreme toxicity and its role in producing harmful tropospheric ozone. It has been shown that the relative atmospheric abundance of O_3 to CO could be an indicator of ozone production environment since positive O_3-CO correlations and regression slopes ($\Delta O_3/\Delta CO$) are identified with ozone production in a place while negative correlations are associated with ozone removal by chemical processes or deposition and/or stratospheric subsidence (Parrish *et al.*, 2000).

The potentially carcinogenic aromatic hydrocarbon, benzene, is a common pollutant in the refinery atmosphere as a result of its presence in crude oil, and as a byproduct of refining operations (van Wijngaarden and Stewart, 2003). While monitoring of human occupational exposures to benzene in the petroleum refining industry is done extensively, its effects on the ecology is a relatively unexplored area (Gaffney *et al.*, 2009). Similarly, polycyclic aromatic hydrocarbons (PAH) usually found in the particulate phase in ambient air in and near an oil refinery have high toxicity for organisms due to their carcinogenic and mutagenic potential. Their effects on flora and fauna have not also been adequately documented (Venturini and Tommasi, 2004).

While vegetation has been known to improve air quality in several ways, there is a tolerance limit beyond which vegetation damage has been quite well-known. Trees are good interceptors of atmospheric pollutants including PM and the gases and they help in regulating atmospheric temperature by lowering air temperature through transpiration. This process affects the photochemistry of formation of ozone in the lower atmosphere (Escobedo *et al.*, 2008; Cardelino and Hameides, 1990).

Acute lower respiratory infections (ALRI), including pneumonia and bronchiolitis have been directly attributed to outdoor air pollution and the diseases arising from bacterial and viral loads of suspended particulates are known as the largest single cause of mortality among young children worldwide under the age of 5 years, representing a significant global burden of disease, 90% of the ALRI deaths being from pneumonia due to outdoor air pollution (Mehta *et al.*, 2013). According to estimates of the World Health Organization (WHO), exposure to urban outdoor $PM_{2.5}$ could have caused approximately 25,600 deaths annually and this can be accounted for by the loss of over 862,000 years of healthy life in 2000 (Cohen *et al.*, 2004).

The present work makes an assessment of the gases, NO_2, SO_2, CO, O_3, NH_3 along with coarse and fine particulates (PM_{10} and $PM_{2.5}$) by active sampling in and around the three million tonne Petroleum Refinery at Numaligarh, India. The Petroleum Refinery is at an aerial distance of 20-25 km from the Kajiranga National Park, a world heritage site and habitat for the vulnerable one-horned rhinoceros. After the establishment of the Refinery, various activities including traffic volume have increased several fold in the area and the environmental situation has deteriorated.

2. MATERIALS AND METHODS

2.1 Study Area

The study area is located at a distance of 32 km from Golaghat (26°38′N, 93°45′E) in Assam, India. The traffic and communication network has improved following the establishment of an oil refinery, resulting in increasing population density and a dense urban and infrastructural network. The Kajiranga National Park lies in the northwestern direction from the refinery. The forest cover of the area is estimated at 60% of the total study area (3505 km^2).

The area is characterized by tropical humid climate with a distinctive summer from May to August and winter from November to January. Moderate climate prevails in the rest of the year. The annual daily average temperature has a moderate value of 25°C, but the maximum temperature during the summer can go up to 34-35°C and the minimum temperature during the winter can go down to 11-13°C (Table 2). Monsoon flourishes during the months of June-August with heavy rainfall through the region. The region becomes more humid due to rainfall continuing till the month of
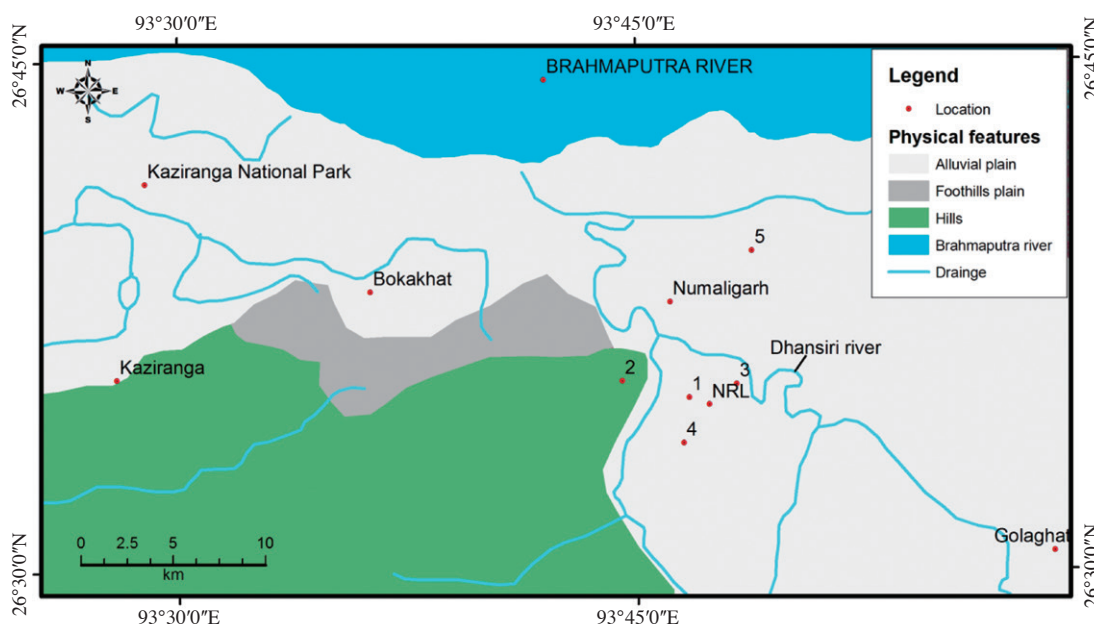
Fig. 1. Map of the study area showing the five air quality sampling locations.

Table 1. Locations of air quality monitoring stations (Direction and distance are from the Refinery main entrance).

Name	Description	Direction	Distance (km)	Coordinates
S1	Near the main entrance of the Refinery	−	0	26°35′2.3″N, 93°46′42.7″E
S2	Near the Refinery Township	N	2	26°35′31.5″N, 93°44′41.5″E
S3	Near the Raw Water Intake Point on the Bank of the Dhansiri River	E	2	26°35′25.3″N, 93°48′23.1″E
S4	At the Highway bypass	S	4	26°33′42.1″N, 93°46′35″E
S5	Kajiranga National Park	NW	25	26°39′17.7″N, 93°48′47.3″E

October. The relative humidity is high throughout the year and the average values remain in the range of 63.2-78.8 mm, the higher values are observed during the hot summer monsoon period (i.e. from month of June to August) when the atmosphere is loaded with water vapour. The prevailing wind direction is north north east (NNE) followed by south east (SE). The wind speed throughout the year remains in the range of 0.0-14.1 km/hr.

2.2 Sampling Locations

Ambient air quality was monitored continuously at pre-determined intervals (9 measurements per month on 24 h/8 h basis) at five locations (S1-S5) throughout a year. Four of the locations were within 10 km radial distance of the Refinery and the fifth one was close to the National Park (Fig. 1). The GPS coordinates of the five locations are given in Table 1. The selection of locations, air quality parameters and the sampling techniques follow the guidelines of Central Pollution

Control Board, Ministry of Environment, Forests and Climate Change, Government of India (CPCB, 2009).

2.3 Sampling and Analysis

The samples were collected with $PM_{10}/PM_{2.5}$ samplers (EcoTech Model AAS 127) equipped with Flow Totalizer and Gas Sampler Assembly (EcoTech Model AAS 118) for collecting SO_2, NO_2, NH_3 and O_3 in ambient air. $PM_{2.5}$ was collected in pre-weighed PTFE filter papers (Whatman, Pore Size 2 μm, diameter 46.2 mm supported on PP rings) while PM_{10} was retained in 47 mm diameter GF/A filter papers (Whatman). The samplers were placed at sites without any physical obstruction on built platforms of ~5 m high above ground level such that vehicle-blown road dusts could be avoided from being collected.

The samplers suck air at a high flow rate of 1.1-1.7 m^3/min through the appropriate filter paper that retains the particles. Ambient air enters the system though an omni directional inlet designed to provide a clean

Table 2. Spatial (5 sites) and monthly (12 months) variations of average values of SO_2, NO_2 and CO around the Numaligarh Oil Refinery (9 measurements each month for each parameter; SO_2 and NO_2 24-hourly; CO 8-hourly) along with basic statistics.

Basic statistics	SO_2 (μg m^{-3})					NO_2 (μg m^{-3})					CO (mg m^{-3})				
	S1	S2	S3	S4	S5	S1	S2	S3	S4	S5	S1	S2	S3	S4	S5
Minimum	2.9	0.7	0.1	1.9	0.0	5.3	2.9	2.2	4.3	2.5	0.3	0.1	0.1	0.2	0.0
Maximum	14.3	5.5	3.6	9.9	2.9	10.5	6.1	4.0	6.7	4.0	0.6	0.3	0.2	0.7	0.1
Mean	9.2	3.7	1.7	6.2	1.1	7.2	4.2	3.1	5.6	3.0	0.4	0.2	0.2	0.4	0.1
Median	8.5	4.2	1.7	7.0	0.9	6.7	4.0	3.0	5.7	2.9	0.4	0.2	0.2	0.4	0.1
Std. Dev.	4.0	1.8	1.0	2.8	1.1	1.7	1.0	0.6	0.9	0.5	0.1	0.1	0.1	0.1	0.0
95 percentile	13.9	5.5	3.2	9.8	2.7	10.5	6.1	3.9	6.7	3.8	0.5	0.3	0.2	0.5	0.1

aerodynamic cut point for particles > 10 μm while the particles of size < 10 μm in diameter proceed to a second impactor that has an aerodynamic cut point at 2.5 μm. The air sample and fine particulates exiting from the $PM_{2.5}$ impactor pass through 47 mm diameter PTFE filter paper for retaining the fine particles. The instrument measures the volume of air sampled, while the amount of particulates collected is determined by measuring the change in weight of the filter paper prior to and after sampling. PM concentration is determined from the formula.

$$PM\,(\mu g\,m^{-3}) = (W_2 - W_1) \times 10^6 / \{(Q_1 + Q_2)/2\} \times time \tag{1}$$

where, W_2 is the weight of the filter paper after sampling (g), W_1 is the weight of the fresh filter paper (g), Q_1 is the initial sampling rate (m^3/min), Q_2 is the final sampling rate (m^3/min).

The Gas Sampler Assembly (EcoTech Model AAS 118) is equipped with provisions for using ice or cold water bath around impingers to prevent heating up of the absorbing solutions due to heat from the blower for ensuring complete absorption of the sparsely soluble gases. Air flow rate into the impingers is controlled at 0.5 to 1.1 m^3/min.

Analysis of the gases in ambient air (SO_2, NO_2, CO, O_3 and NH_3) was done following standard methods (CPCB, 2009; Cetin *et al*., 2007). Modified West and Gaeke method was followed for determination of sulphur dioxide (SO_2) with 0.04 M potassium tetrachloro-mercurate (TCM) solution (30 mL) as the absorbing solution. The resulting dichlorosulphito-mercurate complex was allowed to react with 2 mL para-rosaniline and 2 mL 2% formaldehyde to form intensely coloured pararosaniline methyl sulphonic acid and the absorbance of the solution was measured at 560 nm with a spectrophotometer (Shimadzo UV1800). The concentration of SO_2 was determined with the help of a calibration curve obtained under similar conditions with aqueous sodium sulphite solutions (standard for SO_2) of at least 5 different concentrations in a comparable range.

Modified Jacob and Hochheiser method is used for determining nitrogen dioxide (NO_2) as a measure of NO_x in ambient air. The gas was absorbed as nitrite in an aqueous solution of sodium hydroxide and sodium arsenite, obtained by dissolving 4.0 g of the former and 1.0 g of the latter (1.0 g) in 1000 mL of water. 10 mL of the sampling solution was allowed to interact with 10 mL of a mixture (containing 50 mL 85% phosphoric acid, 20 g sulphanilamide and 1.4 mL of N-1-naphthyl-ethylene diammine dihydrochloride (NEDA) in 1000 mL water) to form an intensely coloured azo dye whose concentration was measured at 540 nm with a UV-visible spectrophotometer (Shimadzo UV1800).

Carbon monoxide (CO) in ambient air was measured directly using Serinus 30 CO analyzer (EcoTech, India) (lowest detection limit < 0.05 mg m^{-3}, range 0-200 mg m^{-3}) with air flow rate of 1000 cm^3/min.

Ozone (O_3) in ambient air was collected by absorbing in 30 mL of aqueous 1% potassium iodide solution buffered at pH 6.8 in a glass impinge in sampler and the tri-iodide formed by the released iodine in 10 mL the solution was measured spectrophotometrically (Shimadzo UV1800) at 352 nm. The ozone content was obtained from a standard calibration curve.

Ammonia (NH_3) in the atmosphere was collected with a glass impinger containing 30 mL of 0.1 N sulphuric acid leading to formation of ammonium sulphate. 10 mL of the solution was allowed to react with 45% (v/v) phenol and 0.1 N alkaline sodium hypochlorite in the presence of 2% sodium nitroprusside as catalyst to produce the dye, indophenol blue, which was estimated spectrophotometrically (Shimadzo UV1800) at 630 nm. Ammonia contents were obtained with the help of a 5 point calibration curve.

3. RESULTS AND DISCUSSION

3.1 Pollutant Variability

Variability diagrams of average spatial concentrations of SO_2, NO_2, CO, O_3, NH_3, PM_{10} and $PM_{2.5}$ (each 9 times a month on 24-hourly basis, ozone and carbon

Fig. 2. Spatial and monthly trends in the average SO_2 contents at five locations.

Fig. 3. Spatial and monthly trends in the average NO_2 contents at five locations.
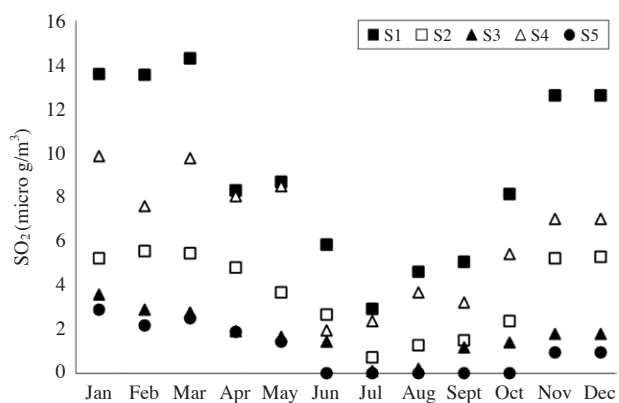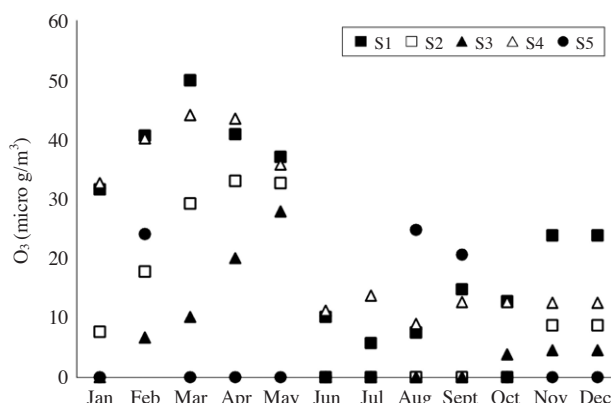

Fig. 4. Spatial and monthly trends in the average CO contents at five locations.

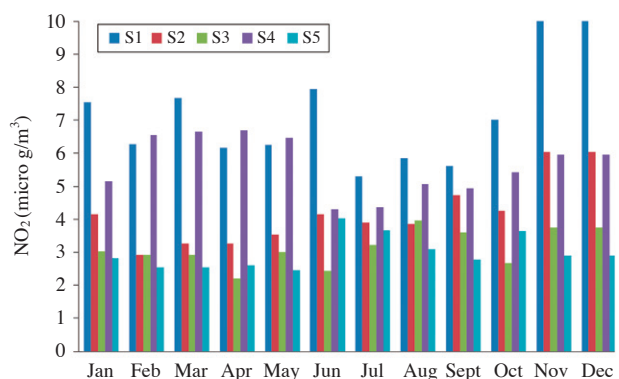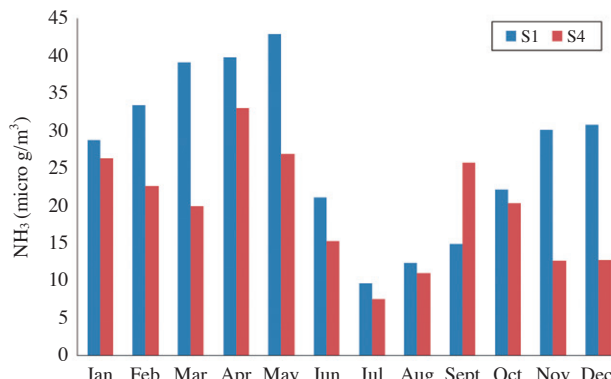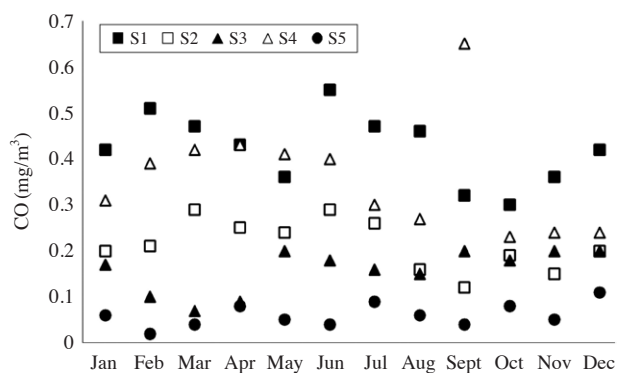**Fig. 5.** Spatial and monthly trends in the average O_3 contents at five locations.

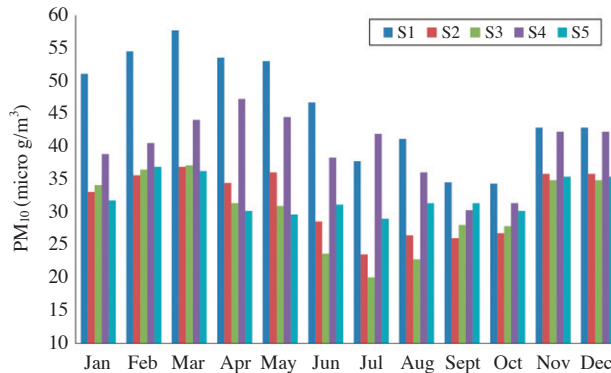**Fig. 6.** Spatial and monthly trends in the average NH_3 contents at five locations.

Fig. 7. Spatial and monthly trends in the average PM_{10} contents at five locations.

monoxide 8-hourly basis) at the sampling sites are given in Figs. 2-8. The average data along with basic statistics are shown in Tables 3-5.

3.2 Concentrations of Sulphur Dioxide

During the wet months of May to September, sulphur dioxide concentrations showed a decreasing trend at all the five sites as frequent rains during this period

washes away SO_2 from the atmosphere (Fig. 2). Even during this time, the sites show some significant differences, with S1 (close to the refinery) and S4 (highway with large traffic volume) recording much higher contents. The overall variations for the five sites for the 12-monthly period are S1: 2.9-14.3 µg m^{-3} (standard deviation, std dev: 4 µg m^{-3}, 95 percentile: 13.9 µg m^{-3}), S2: 0.7-5.5 µg m^{-3} (std dev: 1.8 µg m^{-3}, 95 percentile: 5.5 µg m^{-3}), S3: 0.1-3.6 µg m^{-3} (std dev: 1 µg m^{-3}, 95 percentile: 3.2 µg m^{-3}), S4: 1.9-9.9 µg m^{-3} (std dev: 2.8 µg m^{-3}, 95 percentile: 9.8 µg m^{-3}) and S5: 0.0-2.9 µg m^{-3} (std dev: 1.1 µg m^{-3}, 95 percentile: 2.7 µg

m^{-3}). The median, standard deviation and 95-percentile values were also the highest at the site, S1 followed by S4. These results indicate that most of the gas, SO_2, was generated by the Refinery emissions (S1) and the highway traffic (S4). The concentrations peaked during November to March, when there was almost no rain.

The maximum concentration of 14.30 µg m^{-3} (S1, March) of SO_2 from all the sets of measurements did not exceed the maximum permissible value (80 µg m^{-3}) prescribed in the National Ambient Air Quality Standards (NAAQS), Ministry of Environment, Forests and Climate Change (MoEFCC), Government of India. Sulphur dioxide levels at all the sites are definitely affected by the meteorological conditions as well as by closeness to the Refinery or the traffic congestion points. The relatively higher concentrations of SO_2 at both S1 and S4 during the summer are not only related to the emissions from the refinery and vehicles, but may also be contributed by various smaller sources such as tea and brick factories in the area.

To estimate the possible sources of high winter SO_2 levels, the effects of wind directions during the sampling period were assessed. The non-negligible wind from the north-northeast in April to June might have transported the pollutants northward from the Refinery to the site, S2 (Refinery township) in the south and the southwest wind might have taken the pollutants southward from the Refinery to the site, S3 (near the river Dhansiri), thus distributing SO_2 and other pollutants.

Fig. 8. Spatial and monthly trends in the average PM$_{2.5}$ contents at five locations.

Table 3. Spatial (5 sites) and monthly (12 months) variation of average values of O_3, and NH_3, around the Numaligarh Oil Refinery (9 measurements each month for each parameter; O_3 8-hourly; NH_3, 24-hourly) along with basic statistics.

Basic statistics	O_3 (µg m^{-3})					NH_3 (µg m^{-3})				
	S1	S2	S3	S4	S5	S1	S2	S3	S4	S5
Minimum	5.7	BDL	BDL	8.9	BDL	9.7	BDL	BDL	7.5	BDL
Maximum	49.9	33.0	27.9	44.0	24.8	42.8	BDL	BDL	33.0	BDL
Mean	24.9	11.5	6.5	23.4	5.8	27.1	BDL	BDL	19.5	BDL
Median	23.8	8.2	4.2	13.2	BDL	29.4	BDL	BDL	20.1	BDL
Std. Dev.	15.0	13.3	9.0	14.4	10.5	11.1	BDL	BDL	7.7	BDL
95 percentile	45.0	32.8	23.6	43.8	24.4	41.2	BDL	BDL	29.6	BDL

Table 4. Spatial (5 sites) and monthly (12 months) variation of average values of PM$_{10}$ and PM$_{2.5}$ around the Numaligarh Oil Refinery (9 measurements each month for each parameter; PM$_{10}$ and PM$_{2.5}$ 24-hourly) along with basic statistics.

Basic statistics	PM$_{10}$ (µg m^{-3})					PM$_{2.5}$ (µg m^{-3})				
	S1	S2	S3	S4	S5	S1	S2	S3	S4	S5
Minimum	34.4	23.6	20.1	30.2	29.0	22.0	17.6	16.1	23.6	15.1
Maximum	57.7	36.9	37.1	47.3	36.9	34.1	26.5	23.1	35.1	25.2
Mean	45.9	31.6	30.2	39.8	32.4	28.6	22.4	19.8	29.6	21.4
Median	44.8	33.8	31.2	41.2	31.3	30.8	22.1	19.6	31.0	21.4
Std. Dev.	8.1	4.9	5.7	5.2	2.8	4.5	2.9	2.4	3.8	2.7
95 percentile	56.0	36.4	36.8	45.7	36.5	34.1	26.3	23.1	35.0	25.2

Table 5. Annual mean values of CO, NO_2, O_3, PM_{10}, $PM_{2.5}$ and the enhancement ratios, $\Delta O_3/\Delta CO$, $\Delta O_3/\Delta NO_2$ and $\Delta PM_{10}/\Delta PM_{2.5}$ (obtained from the slopes of the plots of monthly mean values; the monthly means were obtained from 9 measurements each month).

Location	Mean CO ($mg\,m^{-3}$)	Mean NO_2 ($\mu g\,m^{-3}$)	Mean O_3 ($\mu g\,m^{-3}$)	Mean PM_{10} ($\mu g\,m^{-3}$)	Mean $PM_{2.5}$ ($\mu g\,m^{-3}$)	$\Delta O_3/\Delta CO$	$\Delta O_3/\Delta NO_2$	$\Delta PM_{2.5}/\Delta PM_{10}$	Land use type
S1	0.4	7.2	24.9	45.9	28.6	+0.81	−0.48	+0.76	Industry
S2	0.2	4.2	11.5	31.6	22.4	+0.82	−0.72	+0.81	Residential and urban
S3	0.2	3.1	6.5	30.2	19.8	+0.13	−0.40	+0.69	River and residential urban
S4	0.4	5.6	23.4	39.8	29.6	+0.93	+0.69	+0.92	Residential and urban
S5	0.1	3.0	5.8	32.4	21.4	−0.59	−0.27	+0.30	Plain landform/forest

The site, S1, near the Refinery was having much more impact of the dry weather leading to local accumulation of the pollutants, helped by calm conditions. Thus, the spatial variation in SO_2 concentration from one site to another was wide. Further, fuels such as coal and firewood used predominantly over LPG for residential cooking and heating, also contribute to high SO_2 levels in the winter, causing high winter concentrations as compared to the summer values (Cetin *et al.*, 2007). The conditions related to the industrial processes and the traffic do not change significantly with season, and therefore, the decreases in the SO_2 levels in the summer could be attributed to washout effects of the monsoon rain (McGill *et al.*, 1978).

3.3 NO_2 Concentrations

NO_2 showed an identical monthly variation pattern and the site, S1, had the highest monthly concentration of $10.5\,\mu g\,m^{-3}$ during November and December and the lowest monthly concentration of $5.3\,\mu g\,m^{-3}$ during July (Table 2). These concentrations do not exceed the target level of $80\,\mu g\,m^{-3}$ (National Ambient Air Quality Standards, NAAQS, of the Ministry of Environment, Forests and Climate Change, MoEFCC, Government of India). All the other sites have comparatively lower values as shown in Fig. 3. It is seen that NO_2 varied in a narrow range of 5.3 to $10.5\,\mu g\,m^{-3}$, with a median value of $6.7\,\mu g\,m^{-3}$, standard deviation of $1.7\,\mu g\,m^{-3}$, and 95 percentile value of $10.5\,\mu g\,m^{-3}$ at the site, S1.

The trends in the values of SO_2 and NO_2 were similar, because both originated mainly from the combustion of fossil fuels in vehicles, residential heating, chemical processes in the Refinery, etc. Due to the smallness of the area and comparatively large vehicle population density of 5000 vehicles/day on National Highway 37 bypass (S4), 3000 vehicles/day near the township (S2), and 2400 vehicles/day on the road to the refinery (S1) (GT, 2013), the ambient air quality in the area is having a large load of the pollutants when compared to an area away from industrial activities and high traffic. The differences in the concentrations of SO_2 and NO_2 among the five sites may be attributed to spatial and temporal variations in chemical, dispersion, and dilution processes. During the day-light hours, the NO_2-NO inter-conversion complicates NO_2 distribution in the ambient air and it has been shown that NO_2 concentrations have a heterogeneous distribution with a general tendency to accumulate in industrial areas where the conversion is compensated by continuous production (Cetin *et al.*, 2007). This is in agreement with the higher concentrations observed at S1. Natural gas combustion in the industrial plants is recognized as the most significant source of NO_x pollution (Isaksen *et al.*, 2009) and petroleum refining, brick industries, and tea industry are likely to be the major NO_x sources in the study area.

3.4 Variations in Carbon Monoxide

Carbon monoxide concentrations varied between 0.0-$0.5\,mg\,m^{-3}$ in the summer and 0.0-$0.4\,mg\,m^{-3}$ in the winter at the site, S1. Spatial and monthly trends in the average CO contents over the five sampling sites were shown in Fig. 4. The most important sources of CO could be attributed to burning of fuels in the Refinery, in the vehicles and in the nearby tea gardens. The maximum CO concentration of $0.6\,mg\,m^{-3}$ was measured at S4 (Std. Dev. 0.1 and 95 percentile value $0.5\,mg\,m^{-3}$) (Table 2) in September and despite being a considerable value, it still constitutes about one-third of the maximum permissible limit of $2\,mg\,m^{-3}$ (National Ambient Air Quality Standards, India). Higher CO at the site, S4, might have resulted from vehicular emissions in the adjacent motorway and weak wind. During this period, the mean values, the standard deviations and the 95 percentile values of CO at S2 were $0.2\,mg\,m^{-3}$, 0.1 and 0.3 respectively. CO at S2 was low in all the seasons because of wind blowing from the north to northeast direction. The site, S3, had mean CO of $0.2\,mg\,m^{-3}$ with std dev of 0.1, 95 percentile value of 0.2. The site, S5, close to the National Park, as a whole, had very little or no CO. Similar values have been recorded at S1 (mean $0.4\,mg\,m^{-3}$, std dev: 0.1, 95 percentile $0.5\,mg\,m^{-3}$).

CO levels have been observed to be generally high

during the hot, humid months of June and July while the values were lower during the winter. There may be several reasons for this seasonal trend. Air turbulence during the dry months of the winter (Oct to Jan) might have resulted in wider distribution of CO lowering the values. The contributions from biomass burning (paddy fields after harvest were mostly set fire by the farmers to make them ready for the next cultivation) during this period were also likely to be quickly dissipated. Similar trends have been observed by other workers (Edwards *et al*., 2006). The generation of photochemically produced OH radicals is likely to be much more during the day-time in the sunny and dry winter months leading to oxidative destruction of many CO molecules by these radicals, further bringing down the CO levels. During the dry winter, the wash-out effects of rains on OH-radicals is also expected to be minimum making them most effective in scavenging CO from the atmosphere.

3. 5 Ozone Concentration Trends

Ozone concentrations were the highest during the months of March (49.9 $\mu g\,m^{-3}$) and April (40.9 $\mu g\,m^{-3}$) at S1 with standard deviation of 15 $\mu g\,m^{-3}$ and 95 percentile 45 $\mu g\,m^{-3}$ (Table 3). The higher values can be due to the meteorological conditions during this period. The months of March-April are characterized by low wind speed and relative humidity as well as infrequent rains and therefore, there is very little dispersal of ozone. The existing understanding of the atmospheric processes with stronger wind diluting pollutant concentration, rainfall washing out pollutants through wet deposition, and higher temperature accelerating the decomposition of ozone, shows that these conditions have not prevailed during March-April and as a result, there might have been an accumulation of ozone in the atmosphere. It has also been shown during March-April, the inversion layer is very close to the earth's surface in the study area preventing vertical dissipation of ozone, an important factor in increasing ozone concentration (Tian *et al*., 2014). Formation of tropospheric ozone by reactions of volatile organic compounds (VOC) with oxides of nitrogen (NO_x) has also been favoured during these months by long periods of sunny weather.

Higher standard deviation in ozone values shows a correspondingly high temporal variability in ozone concentration. It is to be noted that ozone concentration in all the sites throughout the year was < 100 $\mu g\,m^{-3}$, the maximum permissible value prescribed by NAAQS. During these months, the area had a dry spell with no rains and temperature gradually rising, and therefore, ozone build-up in the atmosphere was not surprising. This trend changed after May, when the monsoon rains

dominated the climate leading to lowering of O_3 concentration in the atmosphere. Since ozone formation arises from interaction of solar light on mixtures of NO_x and hydrocarbons in the air, the situation during the rainy months is not suitable for ozone formation due to frequent cloud cover, reduced period of sunlight, low levels of NO_x and hydrocarbons in the atmosphere due to wash-out processes, etc. Although, ozone has been reported as a typical summer pollutant (Ooka *et al*., 2011), the situation was different in the study area and the highest concentrations were found during the dry months of January, February, March and the rising trend was noticed since November.

The annual cycling of ozone in the study area is shown in Fig. 5. It is observed that the ozone levels are generally low at the predominantly residential site, S2 and the forest site, S5. Linear relationships between NO_2 and O_3 in the ambient air could not be established and it is observed that although there was a general trend of increasing O_3 production with increase in NO_2 in the atmosphere, the regression coefficients were too small to derive any meaningful conclusion. Usually, the oxidation of NO to NO_2 by O_3 should result in a depletion of O_3 and an increase in NO (McConnell *et al*., 2006). However, the observed non-linear increasing trends in both NO_2 and O_3 do not support much conversion of NO_2 to NO by O_3. It is to be noted that NO-NO_2 conversion varies diurnally with sunlight and the participation of O_3 in this process is difficult to quantify as NO and NO_2 speciation has not been done. The photochemical efficiency of sunlight varies across seasons and sites, and with intensity of solar radiations (Khodeir, 2009; Tang *et al*., 2006). In months with relatively lower diurnal variations, the more prominent O_3 peaks are apparently obscured by lower peaks in months with relatively higher variations (Roberts-Semple *et al*., 2012). Higher atmospheric temperature during the dry months of March-April might have also promoted the formation of O_3 (Chou *et al*., 2011).

3. 6 Ammonia Levels and Its Variation

The maximum NH_3 concentration of 42.8 $\mu g\,m^{-3}$ and the minimum concentration of 9.7 $\mu g\,m^{-3}$ were recorded at the site, S1 (Table 3), with standard deviation (standard deviation) of 11.1 $\mu g\,m^{-3}$, respectively in the months of May and July. No NH_3 could be measured at the sites, S2, S3 and S5, while the site, S4, corresponding to high traffic density in the National Highway, showed NH_3 in the overall range of 7.5 $\mu g\,m^{-3}$ (July) to 33.0 $\mu g\,m^{-3}$ (April) with standard deviation of 7.7 $\mu g\,m^{-3}$ (Fig. 6).

Ammonium has now been observed to contribute to particle growth in urban environments (Chan and Yao, 2008). Ammonium nitrate is formed in the atmosphere

through the reaction of NH_3 with HNO_3 (from NO_x) and this is shown as a major player in the rapid growth of mist particles over urban areas (Zhu *et al*., 2014). NH_3 is a critical pollutant determining the acid-base reactions related to the nucleation of particulates. Increases in NH_3 emissions have been shown to be responsible for increase in $PM_{2.5}$ concentrations as it facilitates the nucleation of the particulates with SO_2 and NO_x and combination with other pollutants to form larger particles (Li *et al*., 2016; Huang *et al*., 2014).

The study area in this work is surrounded by intensive agricultural production which may be a major source of NH_3 (Gu *et al*., 2015). The concentrations were higher during the months of March to May, which could be attributed to the fertilization season of the tea gardens in the area. Similar observations have been made earlier (Huang *et al*., 2012).

3. 7 PM_{10} and $PM_{2.5}$ Variations

Monthly average and maximum, minimum values of the particulates measured in the study area are illustrated in Fig. 7 and Fig. 8. It was observed that the annual average PM concentration at all the monitoring stations was lower than the standard limit of 100 and 60 μg m^{-3} for PM_{10} and $PM_{2.5}$ respectively in the industrial as well as the residential areas. During March, the monthly average PM_{10} concentration was the highest i.e. 57.70 μg m^{-3} followed by a level 54.5 μg m^{-3} during February. The maximum levels of particulate matter observed during the months of February and March were due to transported dust over long distances and anthropogenic activities (Fisher *et al*., 2010, 2009). From Table 4, the overall variations in PM_{10} for the five sites during the 12-month period are S1: 34.4-57.7 μg m^{-3} (Standard deviation 8.1 μg m^{-3}, 95 percentile 56 μg m^{-3}), S2: 23.6-36.9 μg m^{-3} (Standard deviation 4.9 μg m^{-3}, 95 percentile 36.4 μg m^{-3}), S3: 20.1-37.1 μg m^{-3} (Standard deviation 5.7 μg m^{-3}, 95 percentile 36.8 μg m^{-3}), S4: 30.2-47.3 μg m^{-3} (Standard deviation 5.2 μg m^{-3}, 95 percentile 45.7 μg m^{-3}) and S5: 29.0-36.9 μg m^{-3} (Standard deviation 2.8 μg m^{-3}, 95 percentile: 36.5 μg m^{-3}). The seasonal variations are mainly due to the meteorological factors such as temperature, relative humidity, and wind speed which favour or adversely affect the dispersion of particulate matter. In addition, changes in source emission strength with time also affect these variations.

The overall variations in $PM_{2.5}$ for the five sites during the 12-month period were S1: 22.0-34.1 μg m^{-3} (Std dev: 4.5 μg m^{-3}, 95 percentile: 34.1 μg m^{-3}), S2: 17.6-26.5 μg m^{-3} (Std dev: 2.9 μg m^{-3}, 95 percentile: 26.3 μg m^{-3}), S3: 16.1-23.1 μg m^{-3} (Std dev: 2.4 μg m^{-3}, 95 percentile: 23.1 μg m^{-3}), S4: 23.6-35.1 μg m^{-3} (Std dev: 3.8 μg m^{-3}, 95 percentile: 35 μg m^{-3}) and S5: 15.1-

25.2 μg m^{-3} (Std dev: 2.7 μg m^{-3}, 95 percentile: 25.2 μg m^{-3}). The main anthropogenic sources of the fine particulates, $PM_{2.5}$, in the study area might be confined to vehicular traffic, fossil fuel combustion, and industrial activities that release a large amount of anthropogenic aerosols to the atmosphere.

In addition, the boundary layer mixing height is likely to be lower in the study area during the winter due to the low wind speed (0.1-9.4 km/h) and temperatures (11.3-27.3°C) that trap the pollutants near the ground as a result of temperature inversion. The winter receives much less rainfall in comparison to the summer. As a result, removal of atmospheric particles by wet scavenging is much reduced in winter than in summer (Deshmukh *et al*., 2010; Karar and Gupta, 2006). Thus, higher concentrations of PM_{10} and $PM_{2.5}$ are expected in the winter. Similar seasonal variations in concentrations of PM have been observed in other urban sites in India (Ramachandran and Kedia, 2010; Badarinath *et al*., 2009). Some studies conducted in urban environment have found that in the winter, the PM concentrations were higher, mainly due to larger use of fossil fuels during the winter days (Akyuz and Cabuk, 2009; Chaloulakou *et al*., 2003). These observations agree with the results obtained in the present work where maximum PM was generally observed during the cold winter months.

The higher relative humidity is known to promote reactions leading to secondary particle formation (Cheng *et al*., 2015; Zhou *et al*., 2015). It was observed that the relative humidity was much higher in the study area during the summer season compared to that in the winter season and the high relative humidity could have negatively impacted the accumulation of PM in the ambient air. The emissions from the Refinery, the vehicles and other industries in the area, coupled with low wind speed and high relative humidity, have resulted in higher concentrations of $PM_{2.5}$ and PM_{10} during the months of April and May.

$PM_{2.5}$ is composed of both primary (e.g., elements, element carbon and primary organic aerosol) and secondary components (e.g., sulphate, nitrate, ammonium and secondary organic) and its diffusion and dispersion through the atmosphere is retarded by high relative humidity (Cheng *et al*., 2013). Also, in conditions of higher humidity, $PM_{2.5}$ in the air may form a stable aerosol over a place where dispersion is less (He *et al*., 2011). The formation of these secondary particles is likely to be accelerated by high humidity, increasing solar radiation and temperature (Tiwari *et al*., 2015; Magiera *et al*., 2011). Thus, $PM_{2.5}/PM_{10}$ ratio is influenced by the relative humidity and the wind speed. Higher values of $PM_{2.5}/PM_{10}$ ratio in the summer could be attributed to the low wind speed and high relative
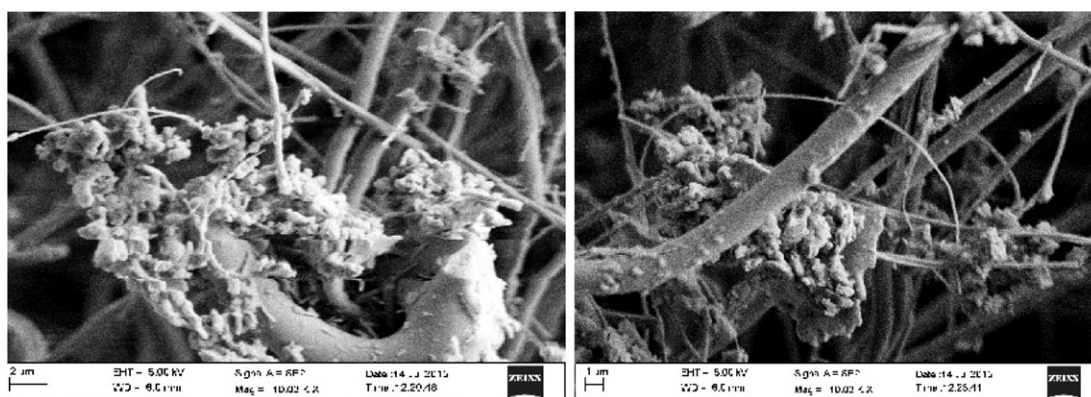
Fig. 9. Scanning electron micrograph of coarse (PM$_{10}$) particulates.
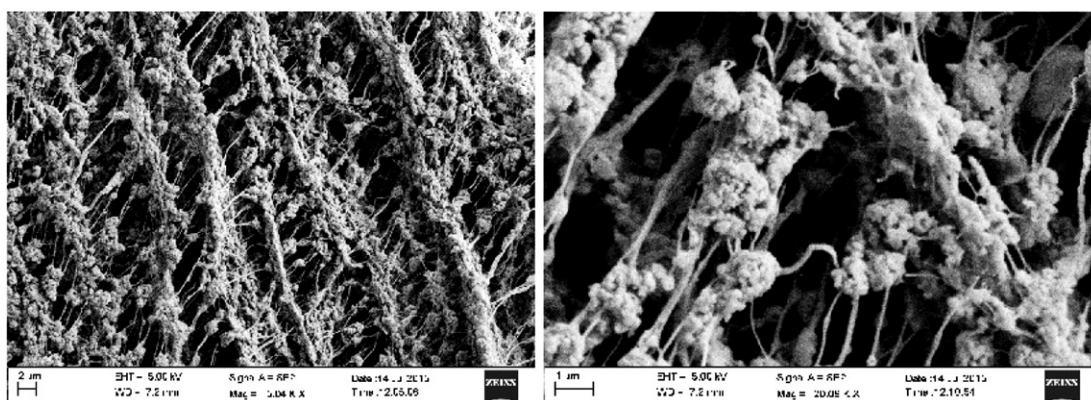

Fig. 10. Scanning electron micrograph of fine (PM$_{2.5}$) particulates.

humidity.

SEM micrographs of coarse and fine particulates (Figs. 9 and 10) were utilised to draw conclusions about their possible origin based on their size and morphological characteristics (Tomasevic and Anicic, 2010). The elongated and irregular shaped particulates observed in the present case indicate that they might have mineral origin (Tomasevic and Anicic, 2010). Some of the particulates, both coarse and fine, are spherical in shape and these could have originated from combustion of fuel. Usually the vehicle engine and the exhaust pipes are the sites for fine particulate generation while the coarse particulates are formed by chemical reactions and by abrasion of the road, tire and brake linings (Palmgren *et al*., 2003). Thus, the origin of most of the aerosol particulates could be traced to emissions from vehicles or from the Refinery.

3.8 Enhancement Ratios

The mean CO, NO$_2$, O$_3$, PM$_{10}$, PM$_{2.5}$ values, obtained on monthly basis (average of nine measurements each month), are given in Table 5 for all the sites. The scatter diagrams obtained by plotting the mean values of one parameter against those of the other were utilized to obtain the parameter-to-parameter enhancement ratios, $\Delta O_3/\Delta CO$, $\Delta O_3/\Delta NO_2$ and $\Delta PM_{10}/\Delta PM_{2.5}$ from the slopes ($\Delta Y/\Delta X$) of the linear best-fit lines (Parrish *et al*., 1993). A large positive enhancement ratio (say, ≥ 0.50 could be considered as equivalent to preponderance of 'Y' over 'X' while a negative enhancement ratio would mean the opposite.

It is observed from Table 6 that the sites, S1, S2 and S4 have significantly large, positive $\Delta O_3/\Delta CO$ (+0.81, +0.82, +0.93 respectively) and therefore, at these sites, O$_3$ will dominate over CO which can be interpreted as resulting from the production of O$_3$ at the cost of CO. It is also possible that at these sites, an oxidative environment exists leading to O$_3$ production while suppressing CO. The site S3 has an insignificantly low enhancement ratio (+0.13) such that both O$_3$ production or CO accumulation are negligible, possibly through a cycle of production, destruction and/or deposi-

Table 6. Air quality index.

Location	AQI value due to a pollutant						IND-AQI	Category	Pollutant responsible
	SO_2 ($\mu g\,m^{-3}$)	NO_2 ($\mu g\,m^{-3}$)	CO ($mg\,m^{-3}$)	O_3 ($\mu g\,m^{-3}$)	PM_{10} ($\mu g\,m^{-3}$)	$PM_{2.5}$ ($\mu g\,m^{-3}$)			
S1	10.12	8.69	20.8	19.95	44.67	47.09	47.09	Good	$PM_{2.5}$
S2	3.85	5.04	10.3	5.11	31.19	37.07	37.07	Good	$PM_{2.5}$
S3	1.55	3.85	7.52	3.46	29.65	32.82	32.82	Good	$PM_{2.5}$
S4	6.83	6.96	17.06	19.50	39.36	47.86	47.86	Good	$PM_{2.5}$
S5	1.54	3.7	2.74	2.19	32.21	35.35	35.35	Good	$PM_{2.5}$

Table 7. SO_2 and NO_2 ratio.

Location	Sampling site	SO_2 ($\mu g\,m^{-3}$)	NO_2 ($\mu g\,m^{-3}$)	SO_2/NO_2
S1	Near the main entrance of the Refinery	9.20	7.22	1.27
S2	Near the Refinery Township	3.65	4.18	0.87
S3	Near the Raw Water Intake Point on the Bank of the Dhansiri River	1.72	3.13	0.55
S4	At the Highway bypass	6.20	5.63	1.10
S5	Kajiranga National Park	1.06	3.00	0.35

tion, resulting in a net loss of ozone to the natural environment (Parrish *et al*., 2000; Fishman and Seiler, 1983). The ratio has a value of −0.59 at the site S5 (mostly forest) and therefore, at this site, the environment is reducing in nature with very little O_3 being generated, while CO production was also very little.

Converting the above results of O_3 production or destruction/deposition to a quantitative frame is much more complicated, however, on the basis of the enhancement ratio, it could be concluded that the sites, S1, S2 and S4 favour ozone production, while the site, S5 might have insignificant ozone either due to its destruction or elimination via deposition. The site S3 cannot be categorised into any of the above two types. The positive O_3-CO correlations at the sites, S1, S2 and S4, are most likely due to transport and subsidence of air with higher O_3 and CO. The two sites, S1 and S4, are likely to have been influenced by a combination of industrial, transport and local urban sources for production of the two gases.

The O_3/NO_x enhancement ratio is negative for the sites, S1 (−0.48), S2 (−0.72), S3 (−0.40) 0 and S5 (−0.27) while it is positive for the site, S4 (+0.69). The tropospheric O_3 formation is associated with long range transport of air masses containing low concentrations of ozone precursors like NO_2. However, as the measurements showed NO_2 concentrations in all the sites are very low and therefore, there may not be appreciable contribution from NO_2 towards ozone production in the whole of the study area. Thus, if the NO_x levels are low, O_3 formation would not be possible resulting in a negative O_3/NO_x enhancement ratio (Delgado, 2004). The negative correlation was the lowest

at the site, S5 near the Kajiranga National Park where both O_3 and NO_2 concentrations were low due to continuous infusion of clean air from the huge green forests on all sides. Contrary to these results, the site, S4, has a positive O_3/NO_x enhancement factor of +0.69, thus disagreeing with the surface correlations existing at the other sites. At this traffic-dominated site, both O_3 and NO_x change unidirectionally giving a considerably large positive enhancement factor.

A similar correlation analysis was attempted to establish relationships between segregated particulate fractions. Such correlations are expected to reveal the consistency of the sources for their emissions. The $\Delta PM_{2.5}/\Delta PM_{10}$ enhancement ratio is positive for all the sites in the range of +0.30 (S5) to +0.92 (S4). The positive values point towards the common sources of origin of fine and coarse particulates. Again, the positive correlation is the largest at the traffic-dominated site, S4 which can be interpreted as indicating that $PM_{2.5}$ particulates in the environment increase nearly linearly with the increase in the coarse particulates, PM_{10}. The variations in the enhancement ratio at the five sites could be explained on the basis of differences in the environmental situation, influence of regional meteorology over local events and sources, etc. Significantly, the $\Delta PM_{2.5}/\Delta PM_{10}$ enhancement ratio is the smallest at S5, close to the National Park where as the measurements have revealed very low $PM_{2.5}$ and PM_{10}, and also the fact that at this site, there is only 30% dependence of $PM_{2.5}$ on PM_{10}.

SO_2/NO_2 ratio (Table 7) can be used to predict the influence of vehicular traffic and industrial emissions, a value <1.0 indicates the vehicular traffic to be dom-

inating influence while a value > 1.0 shows that industrial emissions determine the ambient air quality. In the present work, the ratio is ≤ 1 at all the sites excepting the site, S1, where the ratio is 1.27. Thus, it can be concluded that the contributions to AQI from the moving sources determine the ambient air quality at the sites S2, S3, S4 and S5, while the site S1, close to the Refinery, has maximum contributions from the emissions from various refining units (Deshmukh *et al*., 2010). Further, it is observed that the site, S5, close to the Kajiranga National Park, has SO_2/NO_2 ratio of 0.35 only, indicating that the Petroleum Refinery emissions do not have much say on the aerosol quality, but vehicle movement is the major contributor. Interestingly, the site S4 shows almost equal contributions from vehicular and industrial emissions with SO_2/NO_2 ratio of 1.10.

3.9 Comparative Analysis

Being a relatively under-developed area with green cover all around, PM_{10} and $PM_{2.5}$ measured in this study are expectedly low when compared to those for most of the cities where large amounts of particulates are contributed by traffic emissions, construction and business activities, etc. However, the values compare well to those reported for similar situations. Thus, air quality parameters in very similar ranges have been reported for the religious tourism area of Tirupati, India (Mauli *et al*., 2006). On the other hand, values reported for busy towns and cities are very large compared to those measured in this work. For example, PM_{10} of $231.2\,\mu g\,m^{-3}$ at Korba, $303.8\,\mu g\,m^{-3}$ at Kolkata and $219.0\,\mu g\,m^{-3}$ at Delhi, India are very high to those reported in this work (Deshmukh *et al*., 2010; Tiwari *et al*., 2009; Das *et al*., 2006). $PM_{2.5}$ of $44.0\,\mu g\,m^{-3}$ found at Mumbai (Kothai *et al*., 2008) is comparable to a few of the values in the present work but busy cities like Kolkata (Das *et al*., 2006) and Agra (Kulshrestha *et al*., 2009) in India have very large $PM_{2.5}$ of 178.5 and $170.4\,\mu g\,m^{-3}$ respectively.

The annual concentrations of SO_2 in this work is similar to those reported by Zhou *et al*. (2015) in Beijing ($28.5\,\mu g\,m^{-3}$) but CO, NO_2, O_3, $PM_{2.5}$ and PM_{10} contents of $2.0\,mg\,m^{-3}$, $55.6\,\mu g\,m^{-3}$, $48.0\,\mu g\,m^{-3}$, $92.2\,\mu g\,m^{-3}$ and $118.6\,\mu g\,m^{-3}$, respectively are much higher that what were measured at the study area. On the other hand, the mean CO in the aerosol of Wollongong, Australia ($0.14\,mg\,m^{-3}$) appears to be equal with the concentration measured in this work at the site S5 (Buchholz *et al*., 2016). The ambient concentration of total suspended particulate matter was $34.0\pm4.0\,\mu g\,m^{-3}$ in central Sydney, Australia (Irga *et al*., 2015). It has been found that the sites having large green cover had lower PM_{10} of $19.3\pm4.2\,\mu g\,m^{-3}$, which is also the case with

$PM_{2.5}$ that recorded a value of $19\pm2.1\,\mu g\,m^{-3}$ and $5.3\pm2.0\,\mu g\,m^{-3}$ in sparse and dense forest areas.

In Seoul, Korea, particulate concentration in the city's aerosol was found to be dependent on combustion emissions, crust related sources and heavy traffic activities (Ahmed *et al*., 2016). In a comparison of the ambient concentrations of CO and $PM_{2.5}$ for Beijing, Shanghai, London, Mexico City, Tokyo and New York, it was found that PM_{10} concentration in Beijing ($\sim118\,\mu g\,m^{-3}$) was a little higher than that in Mexico City ($\sim110\,\mu g\,m^{-3}$), but much higher than that in Shanghai ($\sim70\,\mu g\,m^{-3}$) and London ($\sim28\,\mu g\,m^{-3}$). The measurements were, however, made at different times. The SO_2 concentrations found in this work were close to those in London and Tokyo, but lower than those in Shanghai ($\sim23.5\,\mu g\,m^{-3}$) and Mexico city ($\sim28.5\,\mu g\,m^{-3}$). NO_2 contents of the aerosol observed in the present work were in the range of 3.0 to $7.2\,\mu g\,m^{-3}$ only and these values are much less that those in Beijing ($\sim55.6\,\mu g\,m^{-3}$), Shanghai ($\sim45\,\mu g\,m^{-3}$), Tokyo ($\sim46\,\mu g\,m^{-3}$), London ($\sim65\,\mu g\,m^{-3}$) and Mexico city ($\sim78\,\mu g\,m^{-3}$). The large difference might be due to the large number of vehicles in the roads compared to what is there at the study area.

It is clear that if the emission standards for the key sectors are strictly implemented, the situation will improve. Such a scenario has been proposed for China recently by Tang *et al*. (2017).

3.10 Air Quality Index (AQI)

AQI is defined as a numerical rating that reflects the composite influence on overall quality by air quality parameters such that it becomes an important tool for public visualization and urban planning (Bishoi *et al*., 2009). The fundamental advantages of AQI are its simple calculation with a sound scientific basis. The selection of parameters to compute AQI depends upon several factors such as the purpose of the index and the significance of the air quality variables and data variability. The higher the AQI value, the greater is the level of air pollution and the greater the health concerns. An AQI value of 100 is considered as the maximum permissible value with respect to public health. AQI values < 100 will therefore be considered as satisfactory while AQI > 100 will point to unhealthy air quality at least for certain sensitive groups of people, very high AQI will be harmful for all (Mohan *et al*., 2007). The Air quality index is calculated using methodology provided by the Central Pollution Control Board (CPCB) of India. The sub-index values (sub-AQI) for all six air pollutants (PM_{10}, SO_2, NO_x, CO, O_3 and $PM_{2.5}$) are first calculated using the adopted sub-index functions given below. Out of all sub-AQIs, the highest value becomes the overall index and is reported as IND-AQI.
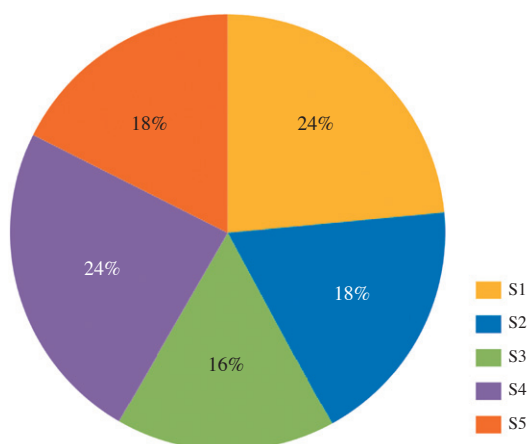
Fig. 11. Air quality index.

The pollutant for which the sub-AQI is the highest, becomes the responsible pollutant, and indicated alongside the IND-AQI value.

The sub-indices are calculated using the equation:

$$q = 100\,(V/Vs) \tag{2}$$

where, q = Quality Rating, V = Observed value of the parameter and Vs = Standard value recommended for the parameter (Chattopadhyay, 2010). The AQI is obtained from the formula:

$$AQI = antilog\,\{(\log q_1 + \log q_2 + ...\log q_x)/n\} \tag{3}$$

where q_1, q_2, q_3, ... q_x are different values of air quality rating, q, for a particular parameter, and n is the number of measurements for which air quality rating is obtained.

Yearly average AQI values in the study area during the one year period are presented in Table 6. The AQI values varied from 1.54 to 47.86 during the study period. High AQI values were estimated mostly in the site S1 and the site S4. The highest AQI values observed in these sites can be attributed to the industrial source, vehicular concentration, massive biomass burning and prevailing meteorological conditions. It is observed that low AQI values characterize the sites, S3 (32.82 $\mu g\,m^{-3}$) and S5 (35.85 $\mu g\,m^{-3}$). PM_{10} and $PM_{2.5}$ are the major pollutants responsible for the deteriorating air quality in the study area emphasizing those aerosol particulates constitute the real environmental problem in the area that is going to present a serious risk to quality of human and animal life.

As shown in Fig. 11, the sites, S1 and S4 contribute 24% each to the total AQI while S2, S3 and S5 contribute 18, 16 and 18% respectively. Highest AQI is 47.86 $\mu g\,m^{-3}$ at site S4, falling under 'good' category, and is not likely to have any detrimental effects on human health. The ratio of concentration to air quality index was highest for $PM_{2.5}$ indicating that $PM_{2.5}$ pollution is going to be a matter of concern in the study area.

4. CONCLUSION

The ambient air quality in the study area was assessed based on the real-time monitoring of concentrations during the period and the meteorological conditions. The annual average concentrations of the principal air pollutants were in the ranges of SO_2: BDL - 14.3 $\mu g\,m^{-3}$, NO_2: 2.2-10.5 $\mu g\,m^{-3}$, CO: BDL - 0.7 $\mu g\,m^{-3}$, O_3: BDL - 49.9 $\mu g\,m^{-3}$, NH_3: BDL - 42.8 $\mu g\,m^{-3}$, PM_{10}: 21.1-57.7 $\mu g\,m^{-3}$, and $PM_{2.5}$: 15.1-35.1 $\mu g\,m^{-3}$ considering all the sites. In all the cases, the values are lower than the national standards prescribed for an ecologically fragile area such as the Kajiranga National Park. Among different types of monitoring stations, the site, S1, near the refinery and the roadside site, S4, had the higher concentrations for all the pollutants.

Background atmospheric pollutant concentration at all the sites was successfully represented by appropriate statistical parameters. The enhancement ratio for the $\Delta O_3/\Delta CO$ correlation shows positive value at the sites, S1, S2, S3 and S4 whereas the correlation is negative at the site S5. The negative trend could be attributed to the differences in the monthly concentration. Similarly $\Delta O_3/\Delta NO_2$ correlation at all the sites shows a negative trend except at the site, S4, where a positive trend with r = 0.63 exists. Correlation analysis between PM_{10} and $PM_{2.5}$ shows a positive trend at all the sites and therefore, reveals a consistency in PM emission.

ACKNOWLEDGEMENT

REFERENCES

Ahmed, E., Kim, K.H., Kim, J., Park, J.K., Chambers, S., Feng, X., Sohn, J.R., Jeon, E.C. (2016) Pollution of airborne metallic species in Seoul, Korea from 1998 to 2010. Atmospheric Environment 124, 85-94.

Akimoto, H. (2003) Global Air Quality and Pollution. Science 302, 1716-1719.

Akyuz, M., Cabuk, H. (2009) Meteorological variations of $PM_{2.5}/PM_{10}$ concentrations and particle-associated polycyclic aromatic hydrocarbons in the atmospheric

environment of Zonguldak Turkey. Journal of Hazardous Materials 170(1), 13-21.

Badarinath, K.V.S., Kharol, S.K., Reddy, R.R., Rama Gopal, K., Narasimhalu, K., Siva Sankara Reddy, L., Raghavendra, K.K. (2009) Black carbon aerosol mass concentration variation in urban and rural environments of India: a case study. Atmospheric Science Letters 10, 29-33.

Bishoi, B., Prakash, A., Jain, V.K. (2009) A Comparative Study of Air Quality Index Based on Factor Analysis and US-EPA Methods for an Urban Environment. Aerosol and Air Quality Research 9, 1-17.

Buchholz, R.R., Paton-Walsh, C., Griffith, D.W.T., Kubistin, D., Caldow, C., Fisher, J., Deutscher, N.M., Kettlewell, G., Riggenbach, M., Macatangay, R., Krummel, P.B., Langenfelds, R.L. (2016) Source and meteorological influences on air quality (CO, CH_4 & CO_2) at a Southern Hemisphere urban site. Atmospheric Environment 126, 274-289.

Cardelino, C.A., Hameides, W.L. (1990) Natural hydrocarbons, urbanization, and urban zone. Journal of Geophysical Research 95(D9), 13971-13979.

Cetin, S., Karademir, A., Pekey, B., Ayberk, S. (2007) Inventory of Emissions of Primary Air Pollutants in the City of Kocaeli, Turkey. Environmental Monitoring and Assessment 128, 165.

Chaloulakou, A., Kassomenos, P., Spyrellis, N., Demokritou, P., Koutrakis, P. (2003) Measurements of PM_{10} and $PM_{2.5}$ particle concentrations in Athens, Greece. Atmospheric Environment 37, 649-660.

Chan, C.K., Yao, X. (2008) Air pollution in mega cities in China. Atmospheric Environment 42, 1-42.

Chattopadhyay, S., Gupta, S., Saha, R.N. (2010) Spatial and Temporal Variation of Urban Air Quality: A GIS Approach. Journal of Environmental Protection 1, 264-277.

Cheng, S.Y., Lang, J.L., Zhou, Y., Han, L.H., Wang, G., Chen, D.S. (2013) A New Monitoring-Simulation-Source Apportionment Approach for Investigating the Vehicular Emission Contribution to the $PM_{2.5}$ Pollution in Beijing, China. Atmospheric Environment 79, 308-316.

Cheng, Y., He, K.B., Du, Z.Y., Zheng, M., Duan, F.K., Ma, Y.L. (2015) Humidity Plays an Important Role in the $PM_{2.5}$ Pollution in Beijing. Environmental Pollution 197, 68-75.

Chou, C.C.K., Tsai, C.Y., Chang, C.C., Lin, P.H., Liu, S.C., Zhu, T. (2011) Photochemical Production of Ozone in Beijing during the 2008 Olympic Games. Atmospheric Chemistry and Physics 11, 9825-9837.

Cohen, A.J., Anderson, H.R., Ostro, B., Pandey, K.D., Krzyzanowski, M., Künzli, N., Gutschmidt, K., Pope, C.A.L., Romieu, I., Samet, J.M., Smith, K.R. (2004) Urban air pollution. In: Ezzati, L.A.M., Rodgers, A., Murray, C.J.L. (eds.), Comparative quantification of health risks: global and regional burden of disease attributable to selected major risk factors, Vol 2. World Health Organization, Geneva, pp. 1153-1433.

CPCB Guidelines for Ambient Air Quality Monitoring. Report under Central Pollution Control Board, Ministry of Environment, Forests and Climate Change, Government of India, 2009.

Das, M., Maiti, S.K., Mukhopadhyay, U. (2006) Distribution of $PM_{2.5}$ and $PM_{10-2.5}$ in PM_{10} fractions in ambient air due to vehicular pollution in Kolkata megacity. Environmental Monitoring and Assessment 122, 111-123.

Delgado, J.M. (2004) Validation and implementation of passive samplers to assess levels and effects of tropospheric ozone and nitrogen dioxide in a Mediterranean coastal area (in Spanish), PhD Thesis, España.

Deshmukh, D.K., Deb, M.K., Tsai, Y.I., Mkoma, S.L. (2010) Atmospheric ionic species in $PM_{2.5}$ and PM_{10} aerosols in the ambient air of eastern central India. Journal of Atmospheric Chemistry 66, 81-100.

Deshmukh, D.K., Deb, M.K., Verma, S.K. (2010) Distribution patterns of coarse, fine and ultrafine atmospheric aerosol particulate matters in major cities of Chhattisgarh. Indian Journal of Environmental Protection 30, 184-197.

Duncan, B.N., Logan, J.A., Bey, I., Megretskaia, I.A., Yantosca, R.M., Novelli, P.C., Jones, N.B., Rinsland, C.P. (2007) Global budget of CO, 1988-1997: Source estimates and validation with a global model. Journal of Geophysical Research 112, D22301.

Edwards, D.P., Emmons, L.K., Gille, J.C., Chu, A., Attie, J.L., Giglio, L., Wood, S.W., Haywood, J., Deeter, M.N., Massie, S.T., Ziskin, D.C., Drummond, J.R. (2006) Satellite observed pollution from southern hemisphere biomass burning. Journal of Geophysical Research: Atmospheres 111(D14), D14312.

Edwards, D.P., Petron, G., Novelli, P.C., Emmons, L.K., Gille, J.C., Drummond, J.R. (2006) Southern Hemisphere carbon monoxide inter-annual variability observed by terra measurement of pollution in the troposphere (MOPITT). Journal of Geophysical Research: Atmospheres 111(D16), D1630.

Escobedo, F.J., Wagner, J.E., Nowak, D., De La Maza, C.L., Rodriguez, M., Crane, D.E. (2008) Analyzing the cost effectiveness of Santiago, Chile's policy of using urban forests to improve air quality. Journal of Environmental Management 86, 148-157.

Fishman, J., Seiler, W. (1983) Correlative nature of ozone and carbon-monoxide in the troposphere e implications for the tropospheric ozone budget. Journal of Geophysical Research: Oceans 88, 3662-3670.

Gaffney, S.H., Panko, J.M., Unice, K.M., Burns, A.M., Kreider, M.L., Gelatt, R.H., Booher, L.E., Paustenbach, D.J. (2009) Occupational exposure to benzene at the Exxon Mobil refinery in Baytown, TX (1978-2006). Journal of Exposure Science and Environmental Epidemiolog 10, 1038.

Gu, B., Ju, X., Chang, J., Ge, Y., Vitousek, P.M. (2015) Integrated reactive nitrogen budgets and future trends in China. Proceedings of the National Academy of Sciences of the United States of America 112, 8792-

8797.

He, K.B., Yang, F.M., Duan, F.K., Ma, Y.L. (2011) Atmospheric Particles and Regional Combined Pollution, Science Press, Beijing.

Heal, K., Kemp, T. (2013) North West Sturgeon Refinery Project Overview - Carbon Capture Through Innovative Commercial Structuring in the Canadian Oil Sands. Energy Procedia 37, 7046-7055.

Huang, R., Zhang, Y., Bozzetti, C., Ho, K., Cao, J., Han, Y., Daellenbach, K.R., Slowik, J.G., Platt, S.M., Canonaco, F., Zotter, P., Wolf, R., Pieber, S.M., Bruns, E.A., Crippa, M., Ciarelli, G., Piazzalunga, A., Schwikowski, M., Abbaszade, G., Schnelle-Kreis, J., Zimmermann, R., An, Z., Szidat, S., Baltensperger, U., Haddad, I.E., Prevot, A.S.H. (2014) High secondary aerosol contribution to particulate pollution during haze events in China. Nature 7521, 218-222.

Huang, X., Song, Y., Li, M., Li, J., Huo, Q., Cai, X., Zhu, T., Hu, M., Zhang, H. (2012) A high-resolution ammonia emission inventory in China. Global Biogeochemical Cycles 26, GB1030.

Irga, P.J., Burchett, M.D., Torpy, F.R. (2015) Does urban forestry have a quantitative effect on ambient air quality in an urban environment. Atmospheric Environment 120, 173-181.

Isaksen, I.S.A., Granier, C., Myhre, G., Berntsen, T.K., Dalsøren, S.B., Gauss, M., Klimont, Z. (2009) Atmospheric Composition Change: Climate-Chemistry Interactions. Atmospheric Environment 43, 5138.

Jaramillo, P., Muller, N.Z. (2016) Air pollution emissions and damages from energy production in the U.S.: 2002-2011. Energy Policy 90, 202.

Kampa, M., Castanas, E. (2008) Human Health Effects of Air Pollution. Environmental Pollution 151, 362-367.

Karar, K., Gupta, A.K. (2006) Seasonal variations and chemical characterization of ambient PM_{10} at residential and industrial sites of an urban region of Kolkata (Calcutta), India. Atmospheric Research 81, 36-53.

Khodeir, M.I. (2009) Diurnal, Seasonal and Weekdays Weekends Variations of Ground Level Ozone Concentrations in an Urban Area in Greater Cairo. Environmental Monitoring and Assessment 149, 349-362.

Kothai, P., Saradhi, I.V., Pratibha, P., Hopke, P.K., Pandit, G.G., Puranik, V.D. (2008) Source apportionment of coarse and fine particulate matter at Navi Mumbai, India. Aerosol and Air Quality Research 8, 423-436.

Kulshrestha, A., Bisht, D.S., Masih, J., Massey, D., Tiwari, S., Taneja, A. (2009) Chemical characterization of water-soluble aerosols in different residential environments of semi arid region of India. Journal of Atmospheric Chemistry 62, 121-138.

Li, L., Kumar, M., Zhu, C., Zhong, J., Francisco, J.S., Zeng, X.C. (2016) Near-barrierless ammonium bisulfate formation via a loop-structure promoted proton-transfer mechanism on the surface of water. Journal of the American Chemical Society 138, 1816-1819.

Logan, J.A., Prather, M.J., Wofsy, S.C., McElroy, M.B. (1981) Tropospheric chemistry: a global perspective. Journal of Geophysical Research: Oceans 86, 7210-7254.

Magiera, T., Jablonska, M., Strzyszcz, Z., Rachwal, M. (2011) Morphological and mineralogical forms of technogenic magnetic particles in industrial dusts. Atmospheric Environment 45, 4281-4290.

Mauli, P.C., Mohan, S.V., Reddy, J. (2006) Chemical composition of atmospheric aerosols (PM_{10}) at a semi-arid urban site: influence of terrestrial sources. Environmental Monitoring and Assessment 117, 291-305.

McConnell, R., Berhane, K., Yao, L., Lurmann, F.W., Avol, E., Peters, J.M. (2006) Predicting Residental Ozone Deficits from Nearby Traffic. Science of The Total Environment 363, 166.

McGill, R., Tukey, J.W., Larsen, W.A. (1978) Variations of Box Plots. The American Statistician 32, 12.

Mehta, S., Shin, H., Burnett, R., North, T., Cohen, A.J. (2013) Ambient particulate air pollution and acute lower respiratory infections: a systematic review and implications for estimating the global burden of disease. Air Quality, Atmosphere & Health 6, 69-83.

Mohan, M., Kandya, A. (2007) An analysis of the annual and seasonal trends of air quality index of Delhi. Environmental Monitoring and Assessment 131, 267-277.

Nishanth, T., Praseed, K.M., Satheesh, K., Vaisaraj, K.T. (2012) Analysis of Ground Level of O_3 and NO_x Measured at Kannur, India. Journal of Earth Science and Climatic Change 3, 1-13.

OECD (2008) OECD environmental performance reviews: Turkey 2008, OECD Publishing (OECD), Paris, France.

Ooka, R., Khiem, M., Hayami, H., Yoshikado, H., Huang, H., Kawamoto, Y. (2011) Influence of Meteorological Conditions on Summer Ozone Levels in Central Kanto Area of Japan. Procedia Environmental Sciences 4, 138.

Palmgren, F., Waahlin, P., Kildeso, J., Afshari, A., Fogh, C.L. (2003) Characterisation of particle emissions from the driving car fleet and the contribution to ambient and indoor particle concentrations. Physics and Chemistry of the Earth, Parts A/B/C 28(8), 327-334.

Parrish, D.D., Holloway, J.S., Jakoubek, R., Trainer, M., Ryerson, T.B., Hübler, G., Fehsenfeld, F.C., Moody, J.L., Cooper, O.R. (2000) Mixing of anthropogenic pollution with stratospheric ozone: a case study from the North Atlantic wintertime troposphere. Journal of Geophysical Research: Atmospheric 105, 24363.

Parrish, D.D., Holloway, J.S., Trainer, M., Murphy, P.C., Fehsenfeld, F.C., Forbes, G.L. (1993) Export of north American ozone pollution to the north Atlantic ocean. Science 259, 1436-1439.

Pudasainee, D., Sapkotab, B., Shresthac, M., Kagac, A., Kondoc, A., Inoue, Y. (2006) Ground Level Ozone Concentrations and Its Association with NO_x and Meteorological Parameters in Kathmandu valley, Nepal. Atmospheric Environment 40, 8081-8087.

Ramachandran, S., Kedia, S. (2010) Black carbon aerosols over an urban region: radiative forcing and climate impact. Journal of Geophysical Research: Atmospheric

doi:10.1029/2009JD013560.

Roberts-Semple, D., Song, F., Gao, Y. (2012) Seasonal Characteristics of Ambient Nitrogen Oxides and Ground Level Ozone in Metropolitan Northeastern New Jersey. Atmospheric Pollution Research 3, 247-257.

Shtripling, L.O., Bazhenov, V.V. (2015) Emission process system organisation of pollutants into the atmosphere for refinery enterprises. Procedia Engineering 113, 349-356.

Tang, Q., Lei, Y., Chen, X., Xue, W. (2017) Air Quality Improvement Scenario for China during the 13th Five-Year Plan Period. Asian Journal of Atmospheric Environment 11(1), 33-36.

Tang, T., Zhang, X.Y., Shao, M. (2006) Atmospheric Environmental Chemistry. Higher Education Press, Beijing.

Tian, G., Qiao, Z., Xu, X. (2014) Characteristics of particulate matter (PM_{10}) and its relationship with meteorological factors during 2001-2012 in Beijing. Environmental Pollution 192, 266-274.

Tiwari, S., Pandithurai, G., Attri, S.D., Srivastava, A.K., Soni, V.K., Bisht, D.S., Kumar, V.A., Srivastava, M.K. (2015) Aerosol Optical Properties and Their Relationship with Meteorological Parameters during Wintertime in Delhi, India. Atmospheric Research 153, 465-479.

Tiwari, S., Srivastava, A.K., Bisht, D.S., Bano, T., Singh, S., Behura, S., Srivastava, M.K., Chate, D.M., Padmanabhamurty, B. (2009) Black carbon and chemical characteristics of PM_{10} and $PM_{2.5}$ at an urban site of North India. Journal of Atmospheric Chemistry 62, 193-209.

Tomasevic, M., Anicic, M. (2010) Trace element content in urban tree leaves and SEM-EDAX characterisation of deposited particles. Physics, Chemistry and Technology 8(1), 1-13.

UNEP (2011) Integrated assessment of black carbon and tropospheric ozone. Summary for decision makers. Nairobi, United Nations Environment Programme.

van Wijngaarden, E., Stewart, P.A. (2003) Critical literature review of determinants and levels of occupational benzene exposure for the United States community based case-control studies. Applied Occupational and Environmental Hygiene 18, 678-693.

Venturini, N., Tommasi, L.R. (2004) Polycyclic aromatic hydrocarbons and changes in the trophic structure of polychaete assemblages in sediments of Todos os Santos Bay, Northeastern, Brazil. Marine Pollution Bulletin 48, 97-107.

Zhou, Y., Cheng, S., Chen, D., Lang, J., Wang, G., Xu, T., Wang, X., Yao, S. (2015) Temporal and Spatial Characteristics of Ambient Air Quality in Beijing, China. Aerosol and Air Quality Research 15, 1868-1880.

Zhu, Y., Sabaliauskas, K., Liu, X., Meng, H., Gao, H., Jeong, C.H., Evans, G.J., Yao, X. (2014) Comparative analysis of new particle formation events in less and severely polluted urban atmosphere. Atmospheric Environment 98, 655-664.